The regular star polymer in the theta state

Fabio Ganazzoli*, Monica A. Fontelos† and Giuseppe Allegra
Dipartimento di Chimica, Politecnico di Milano, Via Mancinelli 7, I-20131 Milano, Italy
(Received 3 June 1992)

The conformation of lightly branched star polymers in the theta state is investigated. Long-range two- and three-body interactions are assumed to compensate one another exactly, whereas the screened interactions, arising from the finite width of the interatomic potential, do survive. Their repulsive potential dies off with interatomic distance r like $\langle r^2\rangle^{-5/2}$, so that the mean-square radius of gyration is asymptotically proportional to the number of bonds N. However, the screened interactions expand the polymer above the random-walk conformation and give rise to a further topology-dependent term proportional to $N^{1/2}$. The topological index $g=\langle S^2\rangle_{star}/\langle S^2\rangle_{lin}$ decreases with increasing N for any degree of branching, becoming linear in $N^{-1/2}$ and tending to the limit $g_\infty=(3f-2)/f^2$ for large N, in agreement with Monte Carlo simulations performed at a vanishing second virial coefficient by Bruns and Carl in 1991. A similar dependence from $N^{-1/2}$ is also found for the ratio of the hydrodynamic radii $h=R_{H,star}/R_{H,lin}$.

(Keywords: star polymers; theta behaviour; interactions; modelling)

INTRODUCTION

An increasing number of experimental results from monodisperse and well characterized regular star polymers have been available in the last few years[1–11] owing to new synthetic methods[1–3,12]. Stimulated by these results, many theoretical papers employing different approaches[7,8,13–18], as well as some Monte Carlo simulations[19–21], have also appeared in the literature. We recently studied[22] the equilibrium properties of regular star polymers in the unperturbed state at the Θ temperature, defined as the temperature at which the second virial coefficient A_2 vanishes. In general, Θ depends on both molecular weight and polymer topology[23–26], although for $N\to\infty$ it tends to the same limit Θ_∞ for any f[4,9,23–25]. Vanishing of A_2 is effectively achieved by compensation between long-range *inter*molecular two- and three-body interactions, the former being attractive and the latter repulsive[23,25,27]. This also implies a virtually complete cancellation between the corresponding *intra*molecular interactions[27]. Therefore, at $T=\Theta$ only shorter-range repulsions contribute to the intramolecular free energy $\mathscr{A}_{intra}$[23,25,28]. In order to distinguish them from the short-range interactions between atoms separated by few chemical bonds, they may be denoted as *medium-range* interactions. They arise from the finite width of the interaction potential, consisting of a hard-core repulsion surrounded by a van der Waals attraction, hence the name 'screened interactions'[28]; they prevent the chain atoms from coming closer than a lower-limit distance, and unlike the long-range interactions they cannot be compensated by solvent-induced attraction at $T=\Theta$. The corresponding free-energy contribution due to two general atoms h and j is proportional to $\langle r^2(h,j)\rangle^{-\gamma}$ with $\gamma=5/2$. Since γ is larger than 2, this potential vanishes quickly with increasing interatomic distance and does not alter the asymptotic proportionality between the mean-square radius of gyration and the molecular weight, but leaves a sizeable effect for finite polymers[23,28]. By contrast, the γ exponent of the long-range interactions is 3/2, and the simple proportionality is lost except at the Θ temperature in the high-molecular-weight limit.

A basic feature of our approach is the representation of the polymer configuration as a sum of Fourier normal modes[23]. The latter were naively derived by analogy with some correct results by Zimm and Kilb dealing with star polymer dynamics[29]. However, after the above-mentioned paper[22] was published, we found that the normal-mode representation employed by us only applies to the so-called phantom polymer, that is, to the polymer devoid of any intramolecular interaction beyond the stereochemical range of a few chemical bonds[23]. As a consequence, most of the results reported[22] were incorrect and the whole paper was therefore withdrawn subsequently[30].

The general normal-mode approach to star polymers was presented by some of us in a recent paper dealing with the good-solvent regime[31]. In the present paper we follow the same approach to study the equilibrium properties in the Θ state. The star will be described by an equivalent bead-and-spring model, with Gaussian distributions for the interbead distances (this is *not* to be confused with a random-walk model, which applies only to the phantom polymer in this context). The effect of first-neighbour correlations among skeletal rotations is absorbed in the effective mean-square length ℓ^2 of the spring connecting adjacent beads; if ν chemical bonds of

* To whom correspondence should be addressed
† Present address: Ausimont SpA, via San Pietro 50, I-20021 Bollate (MI), Italy

0032-3861/93/122615-08

length l are contained within each spring, we have $\ell^2 = vC_\infty l^2$, where C_∞ is the characteristic ratio. For convenience, however, in the following, beads and springs will still be designated as 'atoms' and 'bonds'.

The equilibrium conformation will be determined through self-consistent minimization of the chain free energy[23], written as the sum of an elastic and an interatomic interaction contribution. The former has an entropic origin, opposing any departure from the most probable random-walk conformation, whereas the latter will be regarded as due to the screened interactions only. This approach applies in particular to lightly branched stars; here many-body interactions are of minor importance and the space-filling conditions considered explicitly by some authors[13,14] through scaling theories do not yet apply.

THE NORMAL COORDINATES OF THE REGULAR STAR

The molecule comprises $N+1$ total atoms and f equal branches, hence N/f atoms per branch and one atom at the branch point. A vector $\boldsymbol{\ell}^{(r)}(h)$ is associated with the hth bond of the rth branch, oriented towards the free end; h increases from 1 through N/f from the branch point to the free end. Let us define the vector array $\boldsymbol{L}$ of the bond vectors and the matrix $\boldsymbol{M}$ of the average vector products[23,25]:

$$\boldsymbol{L} = [\boldsymbol{\ell}^{(1)}(1) \quad \boldsymbol{\ell}^{(1)}(2) \quad \dots \quad \boldsymbol{\ell}^{(1)}(N/f) \quad \boldsymbol{\ell}^{(2)}(1) \quad \dots \quad \boldsymbol{\ell}^{(2)}(N/f) \quad \dots \quad \boldsymbol{\ell}^{(f)}(1) \quad \dots \quad \boldsymbol{\ell}^{(f)}(N/f)] \tag{1}$$

$$\boldsymbol{M} = \begin{bmatrix} \boldsymbol{M}_0 & \boldsymbol{M}_1 & \boldsymbol{M}_1 & \dots & \boldsymbol{M}_1 \\ \boldsymbol{M}_1 & \boldsymbol{M}_0 & \boldsymbol{M}_1 & \dots & \boldsymbol{M}_1 \\ \vdots & & & & \vdots \\ \boldsymbol{M}_1 & \boldsymbol{M}_1 & \boldsymbol{M}_1 & \dots & \boldsymbol{M}_0 \end{bmatrix} \tag{2a}$$

where

$$(\boldsymbol{M}_0)_{hj} = \langle \boldsymbol{\ell}^{(r)}(h) \cdot \boldsymbol{\ell}^{(r)}(j) \rangle$$
$$(\boldsymbol{M}_1)_{hj} = \langle \boldsymbol{\ell}^{(r)}(h) \cdot \boldsymbol{\ell}^{(s)}(j) \rangle \qquad r \neq s \tag{2b}$$
$$\langle [\boldsymbol{\ell}^{(r)}(h)]^2 \rangle = \ell^2.$$

Sending the reader to ref. 31 for more details, the normal coordinates $\tilde{\boldsymbol{L}} = [\tilde{\boldsymbol{\ell}}(1), \dots, \tilde{\boldsymbol{\ell}}(N)]$ are obtained from $\boldsymbol{L}$ by:

$$\tilde{\boldsymbol{L}} = \boldsymbol{L} \cdot \boldsymbol{V} \tag{3a}$$

where

$$\boldsymbol{V}^{*\mathrm{T}} \cdot \boldsymbol{M} \cdot \boldsymbol{V} = \boldsymbol{\Lambda} \text{ (diagonal)} \qquad \boldsymbol{V} \cdot \boldsymbol{V}^{*\mathrm{T}} = \boldsymbol{E}_N \tag{3b}$$

$\boldsymbol{E}_N$ being the identity matrix of order N. It is useful to perform the diagonalization in two steps[25,31]. First we reduce $\boldsymbol{M}$ to the block-diagonal form:

$$\boldsymbol{\Lambda}_{\text{block}} = \boldsymbol{X}^* \cdot \boldsymbol{M} \cdot \boldsymbol{X} = \begin{bmatrix} \boldsymbol{M}_0 + (f-1)\boldsymbol{M}_1 & \mathbf{0} & \mathbf{0} & \dots & \mathbf{0} \\ \mathbf{0} & \boldsymbol{M}_0 - \boldsymbol{M}_1 & \mathbf{0} & \dots & \mathbf{0} \\ \mathbf{0} & \mathbf{0} & \boldsymbol{M}_0 - \boldsymbol{M}_1 & \dots & \mathbf{0} \\ \vdots & & & & \\ \mathbf{0} & \mathbf{0} & \mathbf{0} & \dots & \boldsymbol{M}_0 - \boldsymbol{M}_1 \end{bmatrix} \tag{4}$$

where the unitary matrix $\boldsymbol{X}$ is defined as

$$\boldsymbol{X} = f^{-1/2} \begin{bmatrix} 1 & 1 & 1 & \dots & 1 \\ 1 & e^{i\varphi} & e^{2i\varphi} & \dots & e^{i(f-1)\varphi} \\ 1 & e^{2i\varphi} & e^{4i\varphi} & \dots & e^{2i(f-1)\varphi} \\ \vdots & & & & \\ 1 & e^{i(f-1)\varphi} & \dots & \dots & e^{i(f-1)^2\varphi} \end{bmatrix} \otimes \boldsymbol{E} \tag{4a}$$

$$\varphi = 2\pi/f \qquad \boldsymbol{X}^{-1} = \boldsymbol{X}^*$$

$\otimes$ being the symbol for the direct product. The eigenvalues may therefore be collected into two classes: the first one has unit multiplicity and derives from diagonalization of $\boldsymbol{M}_0 + (f-1)\boldsymbol{M}_1$; the second one has multiplicity $(f-1)$ and derives from diagonalization of $\boldsymbol{M}_0 - \boldsymbol{M}_1$. We now assume (i) *conformational uniformity* within the chain, meaning that the average product of two bond vectors only depends on their topological separation, and (ii) *short-range correlations*, meaning that the average bond-vector product vanishes quickly with increasing topological separation. Both requirements are met to a very good degree in the unperturbed state and represent sufficient conditions to have Fourier-type normal modes. By further considering the molecular symmetry and the boundary conditions at the arm ends, $\boldsymbol{M}_0 + (f-1)\boldsymbol{M}_1$ and $\boldsymbol{M}_0 - \boldsymbol{M}_1$ in equation (4) are reduced to the diagonal matrices $\boldsymbol{\Lambda}_A$ and $\boldsymbol{\Lambda}_B$ through the rotation matrices $\boldsymbol{A}$ and $\boldsymbol{B}$, respectively, where:

$$(\boldsymbol{\Lambda}_A)_{mn} = \ell^2 \alpha_m^2 \delta_{mn} \qquad (\boldsymbol{\Lambda}_B)_{mn} = \ell^2 \beta_m^2 \delta_{mn} \tag{5}$$

$$\boldsymbol{A}^{\mathrm{T}} \cdot \boldsymbol{A} = \boldsymbol{E}_{N/f} \qquad \boldsymbol{B}^{\mathrm{T}} \cdot \boldsymbol{B} = \boldsymbol{E}_{N/f} \tag{5a}$$

$$(\boldsymbol{A})_{hm} = C \sin[q_{2m}(h - 1/2)]$$
$$(\boldsymbol{B})_{hm} = C \cos[q_{2m-1}(h - 1/2)] \tag{5b}$$
$$q_p = \pi p/(2N/f + 1) \qquad C = 2/(2N/f + 1)^{1/2}$$

From equations (3)–(5) we have:

$$\tilde{\boldsymbol{L}} = \boldsymbol{L} \cdot \boldsymbol{V} \qquad \boldsymbol{V} = \boldsymbol{X} \cdot \begin{bmatrix} \boldsymbol{A} & & & \\ & \boldsymbol{B} & & \\ & & \boldsymbol{B} & \\ & & & \ddots \\ & & & \boldsymbol{B} \end{bmatrix} \tag{6}$$

and the full expression of the normal coordinates is:

for antisymmetric modes

$$\tilde{\boldsymbol{\ell}}(q_{2m}) = f^{-1/2} C \sum_{h=1}^{N/f} \left(\sum_{r=1}^{f} \boldsymbol{\ell}^{(r)}(h) \right) \sin[q_{2m}(h - 1/2)] \tag{7a}$$

for symmetric modes

$$\tilde{\boldsymbol{\ell}}^{(v)}(q_{2m-1}) = f^{-1/2} C \sum_{h=1}^{N/f} \left(\sum_{r=1}^{f} \boldsymbol{\ell}^{(r)}(h)\, e^{irv\varphi} \right) \cos[q_{2m-1}(h - 1/2)] \tag{7a}$$

where $v = 1, 2, \dots, f-1$; $m = 1, 2, \dots, N/f$.

The mode symmetry may be simply associated with that of the sine and cosine functions, although a more complete justification exists[31]. Since all the $\tilde{\boldsymbol{\ell}}^{(v)}$ sets with different v are statistically equivalent, for brevity we shall only refer in the following to the set with $v = 1$, dropping the v index and suitably accounting for the $(f-1)$

multiplicity. We therefore put:

$$\tilde{\ell}(q_{2m-1}) = \tilde{\ell}^{(v=1)}(q_{2m-1}) \tag{7c}$$

It will be recognized from equations (3)–(6) that the eigenvalues α_m^2 and β_m^2 are the strain ratios of the mean-square antisymmetric and symmetric modes, respectively.

THE FREE-ENERGY SELF-CONSISTENT OPTIMIZATION

We need first the analytical expression of the mean-square interatomic distances between atoms h and j on branches r and s as a function of the strain ratios α_m^2, β_m^2 (see equation (5); $0 \leqslant h, j \leqslant N/f$, 0 being the branch point and N/f the free end). We have[31]:

$$\langle r^2(h,j)\rangle_{rs} = (\ell^2/f) \sum_{m=1}^{N/f} \{(a_{hj}^{(m)})^2 \alpha_m^2 + [(f-1)(b_{hj}^{(m)})^2 + 2f(1-\delta_{rs}) b_{0h}^{(m)} b_{0j}^{(m)}] \beta_m^2\} \tag{8}$$

where

$$a_{hj}^{(m)} = C \sin[q_{2m}(j+h)/2] \sin[q_{2m}(j-h)/2]/\sin(q_{2m}/2) \tag{9}$$

$$b_{hj}^{(m)} = C \cos[q_{2m-1}(j+h)/2] \times \sin[q_{2m-1}(j-h)/2]/\sin(q_{2m-1}/2) \tag{9a}$$

$$q_p = \pi p/(2N/f+1) \qquad C = 2/(N/f+1)^{1/2} \tag{9b}$$

Within the Gaussian approximation, from the mean-square distances we also get the mean-square radius of gyration $\langle S^2 \rangle$ as a function of the strain ratios:

$$\langle S^2 \rangle = [2(N+1)^2]^{-1} \sum_h \sum_j \langle r^2(h,j) \rangle = [4(N+1)]^{-1} \sum_{m=1}^{N/f} \left[\frac{\alpha_m^2}{\sin^2(q_{2m}/2)} \left(1 + \frac{2-f}{N+1}\right) + (f-1) \frac{\beta_m^2}{\sin^2(q_{2m-1}/2)} \right] \tag{10}$$

as well as the hydrodynamic radius R_H:

$$R_H^{-1} = (N+1)^{-2} \sum_h \sum_j \langle r^{-1}(h,j) \rangle$$

$$\langle r^{-1}(h,j) \rangle = [6/\pi \langle r^2(h,j) \rangle]^{1/2} \tag{10a}$$

From the 'Introduction', the free energy in $k_B T$ units is expressed as:

$$\mathscr{A} = \mathscr{A}_{el} + \mathscr{A}_{intra} \tag{11}$$

The elastic component $\mathscr{A}_{el}$ has a purely entropic origin and is given by[25]:

$$\mathscr{A}_{el} = (3/2) \sum_{m=1}^{N/f} [\alpha_m^2 - 1 - \ln \alpha_m^2 + (f-1)(\beta_m^2 - 1 - \ln \beta_m^2)] \tag{12}$$

the multiplicities of the modes with different symmetry being due to the degeneracies of the eigenvalues (see equation (4)). The intramolecular component $\mathscr{A}_{intra}$ is only due to the screened interactions[23,25,28]:

$$\mathscr{A}_{intra} = (1/2) \sum_h \sum_j a_{2S}(h,j)$$

$$a_{2S}(h,j) = K \ell^5 \langle r^2(h,j) \rangle^{-5/2} \tag{13}$$

K being an appropriate non-dimensional parameter proportional to the mean-square chain thickness. In equation (13) the double sum runs over all the star atoms $0 \leqslant h, j \leqslant N$, *provided* they are separated by at least $\bar{k}$ bonds. This lower cut-off[25,28] arises from the intrinsic stereochemical requirements of a real polymer, and its value may be estimated according to the procedure discussed in ref. 25: a typical value of $\bar{k}$ is 50 chemical bonds for atactic polystyrene. In the present context, where an equivalent bead-and-spring model is adopted, $\bar{k}$ decreases by a factor v, where v is the number of chemical bonds per spring.

The equilibrium conformation is obtained by minimization of the overall free energy (equations (11)–(13), together with equation (8)) with respect to all the degrees of freedom, i.e. $\partial \mathscr{A}/\partial \alpha_m^2 = 0$ (antisymmetric modes) and $\partial \mathscr{A}/\partial \beta_m^2 = 0$ (symmetric modes). The resulting equations are:

$$\frac{1}{\alpha_m^2} = 1 - \frac{5}{6} \frac{K}{f} \sum_h \sum_j (a_{hj}^{(m)})^2 J(h,j)^{-7/2} \tag{14}$$

$$\frac{1}{\beta_m^2} = 1 - \frac{5}{6} \frac{K}{f} \left(\sum_h \sum_j (b_{hj}^{(m)})^2 J(h,j)^{-7/2} + \frac{2f}{(f-1)} \sum_h{}' \sum_j{}' b_{0h}^{(m)} b_{0j}^{(m)} J(h,j)^{-7/2} \right) \tag{14a}$$

where

$$J(h,j) = \langle r^2(h,j) \rangle / \ell^2 \tag{14b}$$

the topological separation between h and j never being smaller than $\bar{k}$. In equations (14) the unprimed double sums run over all pairs of atoms, whereas the primed double sum in equation (14a) is performed only on pairs *on different arms*. Equations (14) together with equation (8) form a coupled set of equations to be solved self-consistently.

THE REGULAR STAR POLYMER AT $T = \Theta$

The perturbative approach

We follow first a perturbative approach, assuming K to be small and the arm length very large, i.e. $N/f \gg 1$. We start with the phantom-chain strain ratios $\alpha_m^2 \equiv \beta_m^2 \equiv 1$, hence with $\langle r^2(h,j) \rangle = |h-j| \ell^2$ for atoms on the same arm (see equation (8), $r = s$) or $\langle r^2(h,j) \rangle = (h+j) \ell^2$ for atoms on two different arms ($r \neq s$). Inserting these values in equations (14) and transforming the sums into integrals, we get the perturbative values of α_m^2 and β_m^2. We focus our attention on the collective internal modes having the Fourier coordinate $q_p \ll 1$, i.e. on the large-scale properties, but at the same time we assume $p \propto q_p N/f \gg 1$ ($p = 2m$ or $2m-1$, see equation (5b)). After some straightforward but tedious algebra, we get

$$\alpha_m^2 \simeq \beta_m^2 \simeq \bar{\alpha}^2 - (8/9)(K/\bar{k}^{1/2})(2\pi q_p \bar{k})^{1/2} \tag{15}$$

$$\bar{\alpha}^2 = 1 + (10/3) K/\bar{k}^{1/2} \tag{16}$$

where $p = 2m$ (for α_m^2, antisymmetric modes) or $p = 2m-1$ (for β_m^2, symmetric modes) and terms of the order of $(N/f)^{-1/2} p^{-\varepsilon}$, $\varepsilon \geqslant 1/2$, are neglected; this is warranted if $p \gg 1$, as stated above. Note that equations (15) and (16) give the linear chain result* for $f = 2$ and that the polymer

* The result in equation (15) coincides with that of the linear chain[28] for $f = 2$, if we note that the constant G in ref. 28 is given by $G = (4/15)(2\pi)^{1/2}$

topology does not appear explicitly in equation (15). In the high-molecular-weight limit both α_m^2 and β_m^2 tend to the same constant $\bar{\alpha}^2$ for the collective modes (small m), thus yielding an *asymptotically affine expansion* independent of the number of arms. The present result is consistent with the localized character of the screened interactions; therefore, for $N/f \to \infty$ their effect on the large-scale properties may be absorbed into an effective, renormalized bond length $\bar{\alpha}\ell$, independent of the polymer topology. Thus, for example, the mean-square radius of gyration is asymptotically given by the simple expression:

$$\langle S^2 \rangle = \bar{\alpha}^2 \ell^2 \frac{N}{6} \frac{3f-2}{f^2} \tag{17}$$

More generally, the result reported in equation (15), when inserted into equation (10), implies that an additional term proportional to $N^{1/2}$ is present in $\langle S^2 \rangle$, so that we may write, in analogy with what we found for the linear chain[27,28]:

$$\langle S^2 \rangle = \bar{\alpha}^2 \ell^2 \frac{N}{6} \frac{3f-2}{f^2} [1 - \Delta(f) N^{-1/2}] \tag{17a}$$

where the prefactor $\Delta(f)$ depends on the polymer topology. Its value as well as its sign depend crucially on the strain ratio of the most collective modes with m of order unity, which cannot be evaluated analytically in closed form even to first order in the parameter K. We therefore turned to a numerical solution of the coupled equations (14) and (8).

The full numerical solution

The numerical solution of the full self-consistent equations (14) and (8) was found using the same iterative procedure as we used previously (see e.g. ref. 28). In doing so, no further mathematical approximation is required and short-arm polymers may be easily handled by carrying out the full sums. We chose $K = 0.087$ and a cut-off value $\bar{k} = 1$ for simplicity, so that the effective variable $K/\bar{k}^{1/2}$ has the value already used by us for atactic polystyrene in previous work[28]; the largest f taken into consideration was 12 and the largest arm length was $N/f = 400$. From the self-consistent sets of α_m^2, β_m^2 and $\langle r^2(h,j) \rangle$ values, we get $\langle S^2 \rangle$ and R_H through equations (10). The numerical results are reported in *Figure 1* as $\langle S^2 \rangle / [N\ell^2(3f-2)/f^2]$ as a function of $N^{-1/2}$ for the linear chain ($f=2$) and for nine- and twelve-arm stars. In agreement with equation (17a), the plot is linear at large N, $\Delta(f)$ being positive and largest for $f=2$, then decreasing with increasing f and becoming negative for $f > 4$†. Therefore, for a given N, the ratio $\langle S^2 \rangle / [N\ell^2(3f-2)/f^2]$ is larger the larger is f, because the arms are shorter so that the relative importance of the repulsive interactions across the branch point is larger. Furthermore, *Figure 1* shows that, at smaller N, terms in N^{-1} and higher negative powers of N are non-negligible, imparting a downward curvature to the plots for $f=9$ and 12.

The corresponding plot for the hydrodynamic radius is reported in *Figure 2*, where we show $R_H / \{N^{1/2}\ell f^{1/2} / [2-f+(f-1)\sqrt{2}]\}$ as a function of $N^{-1/2}$. The curves display an upward curvature for both the linear and the star polymer, unlike the curves of $\langle S^2 \rangle$ shown in

† In ref. 25 two of us made the incorrect statement that $\Delta(f)$ is positive and increasing with f. The error must be traced back to the inaccurate extrapolation of equations (15) to the very first modes

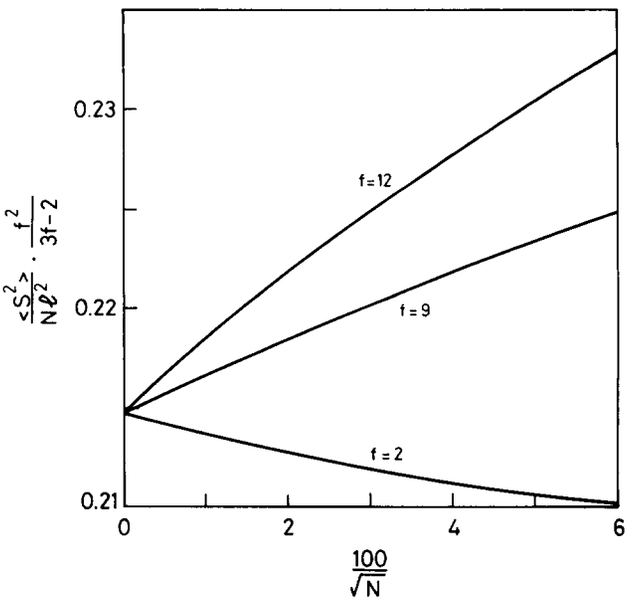

Figure 1 The mean-square radius of gyration plotted as $\langle S^2 \rangle / [N\ell^2(3f-2)/f^2]$ as a function of $N^{-1/2}$ for the linear and the star polymer. The number of arms f is shown on the curves. The common limit of all the curves for $N \to \infty$ is given by $\bar{\alpha}^2/6$ (see also equations (16) and (17))

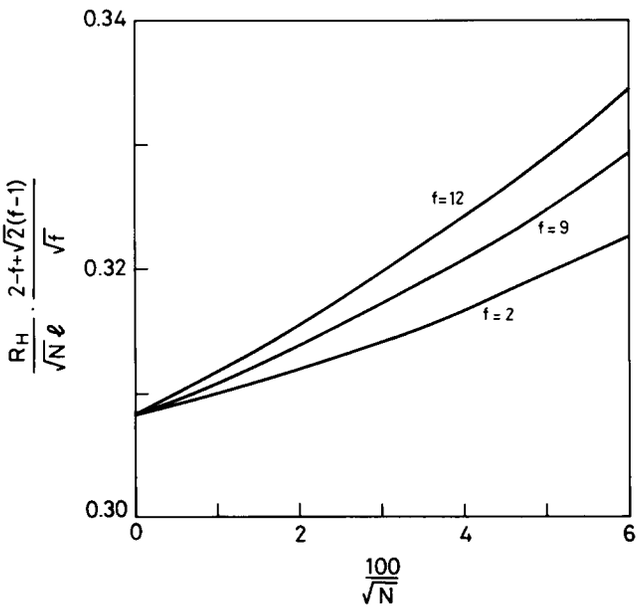

Figure 2 Same as *Figure 1* for the hydrodynamic ratio plotted as $R_H / \{N^{1/2}\ell f^{1/2} / [2-f+(f-1)\sqrt{2}]\}$. The limit for $N \to \infty$ is $\frac{3}{8}(\pi/6)^{1/2}\bar{\alpha}$

Figure 1. In this respect, we point out that relatively short sequences experiencing little, if any, expansion have a larger weight in determining R_H than in $\langle S^2 \rangle$ both because R_H is a linear quantity and because it depends on reciprocal averages (see equation (10a)). Therefore, the screened interactions are less important and the plots of the hydrodynamic radius are qualitatively similar to those of the phantom polymer, unlike those of the mean-square radius of gyration. In particular, for the phantom polymer it may be shown that both $\langle S^2 \rangle / N$ and $R_H / N^{1/2}$ decrease with increasing N because of terms proportional to N^{-1} (see later).

In order to make a better comparison of the present results with those of the phantom polymer, we report in

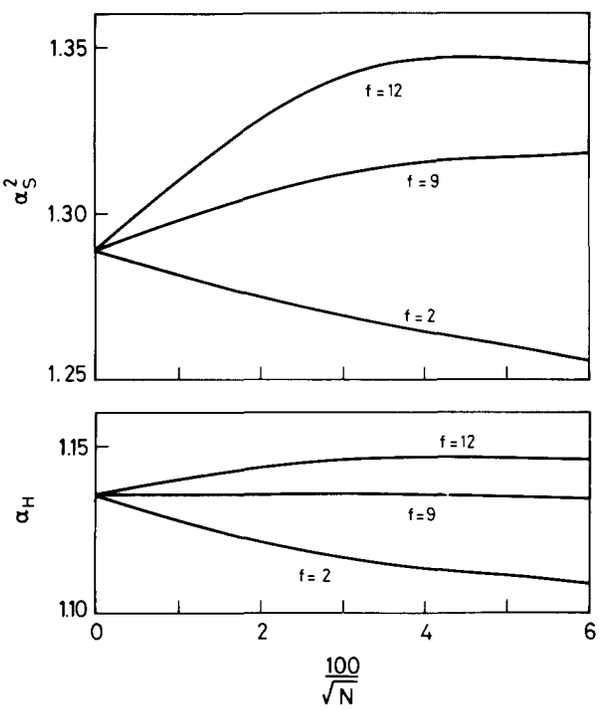

Figure 3 The molecular-weight dependence of ratios $\alpha_s^2 = \langle S^2\rangle/\langle S^2\rangle_{ph}$ and $\alpha_H = R_H/R_{H,ph}$ for the linear and the star polymer (see text)

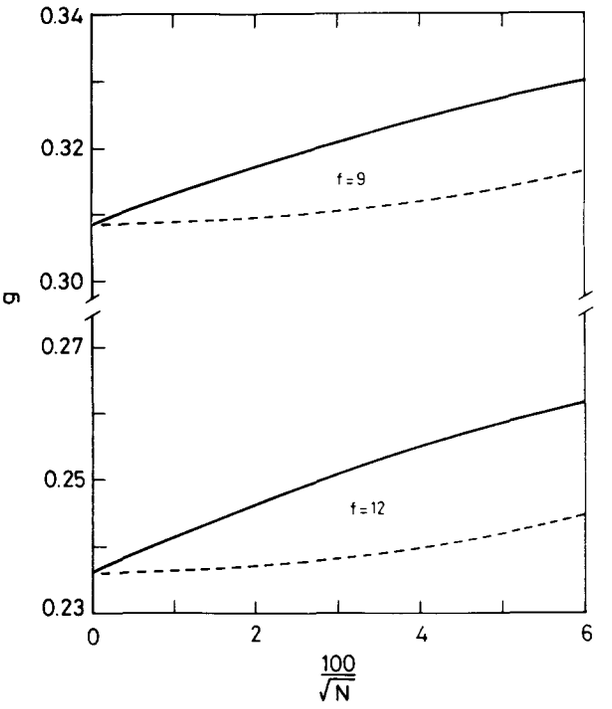

Figure 4 The g ratio $g = \langle S^2\rangle_{star}/\langle S^2\rangle_{lin}$ (see equation (19)) as a function of $N^{-1/2}$ for a nine-arm and a twelve-arm polymer. The limiting value for $N \to \infty$ is given by equation (19a)

Figure 3 the expansion ratios α_S^2 and α_H, defined as:

$$\alpha_S^2 = \langle S^2\rangle/\langle S^2\rangle_{ph} \tag{18}$$

$$\alpha_H = R_H/R_{H,ph} \tag{18a}$$

where the results for the discrete phantom polymer are obtained through equations (8)–(10) and (14) by setting $\alpha_m^2 \equiv \beta_m^2 \equiv 1$. In this case, the curves of the two expansion factors are qualitatively similar: in particular, for the linear chain both α_S^2 and α_H increase with increasing N. This suggests that the different behaviour shown in *Figures 1* and *2* is indeed due to the small expansion of the short strands, which makes R_H less affected than $\langle S^2\rangle$ by the screened interactions. Furthermore, the maximum in the plots for the twelve-arm star is of interest, again reflecting the small expansion experienced by the star with very short arms. An analogous, although shallower, maximum is also shown by the nine-arm star at roughly the same arm length, therefore at a smaller N. This result is in keeping with the notion that the expansion is affine only in the asymptotic limit, but not for finite polymers, as is implicit in equation (17a), whereas short strands comprising few atoms are not affected.

The topological indices

A quantity often reported in the literature is the topological index g, defined as the ratio:

$$g = \langle S^2\rangle_{star}/\langle S^2\rangle_{lin} \tag{19}$$

This index may be taken as a measure of the degree of compactness of the star as compared with the linear chain having the same molecular weight. From the curves reported in *Figure 1*, we get the results shown in *Figure 4* (full curves). Furthermore, equations (17) show that, for $N \to \infty$, g tends to the value[32]:

$$g_\infty = (3f-2)/f^2 \tag{19a}$$

It is remarkable that g tends *from above* to the asymptotic value g_∞ with an $N^{-1/2}$ dependence; in fact, from equation (17a) we have:

$$g \simeq g_\infty\{1 + [\Delta(2) - \Delta(f)]N^{-1/2}\} \tag{20}$$

(we recall that $\Delta(f) < 0$ for $f > 4$). For smaller N, further terms of the order of N^{-1} are non-negligible, which impart a downward curvature to the plots.

In this context, we point out that for the phantom chain we have $\langle r^2(h,j)\rangle = k\ell^2$ throughout, k being the bond separation between atoms h and j ($k = 1, 2, \ldots, 2N/f$). Assuming first a *continuous* contour coordinate k, the sums over h and j in equation (10) are replaced by integrals and we get:

$$\langle S^2\rangle_{ph}^{cont} = g_\infty N\ell^2/6 \tag{21}$$

for *any* N. On the other hand, assuming a *discrete* chain model and performing the sums exactly as done throughout in the present paper, we have:

$$\langle S^2\rangle_{ph}^{discr} = \frac{N\ell^2(N/f+1)}{6(N+1)^2}\left(\frac{N}{f}(3f-2)+2\right) \tag{22}$$

whence

$$g_{ph}^{discr} = \frac{N/f+1}{(N+1)(N+2)}\left(\frac{N}{f}(3f-2)+2\right)$$

$$\simeq g_\infty + 3(1-g_\infty)N^{-1} \tag{23}$$

so that g_{ph}^{discr} decreases with increasing N ($g_\infty < 1$ if $f > 2$, see equation (19a)). The plot of g_{ph}^{discr} is reported for comparison in *Figure 4* (broken curves): the N^{-1} dependence gives a much faster convergence of g_{ph}^{discr} to the asymptotic value g_∞ and a parabolic plot with an upward curvature when reported as a function of $N^{-1/2}$, unlike our results (full curves).

A similar topological index h may be defined in terms of the hydrodynamic radius R_H:

$$h = R_{H,star}/R_{H,lin} \tag{24}$$

From the plots of *Figure 2*, we get the curves reported in *Figure 5* (full curves). For $N \to \infty$, h tends to the limit[33]:

$$h_\infty = \frac{f^{1/2}}{2-f+(f-1)\sqrt{2}} \qquad (24a)$$

equal to the asymptotic value of the phantom polymer. The curves are quite similar to those of the g ratio with a smaller slope at large N; this is consistent with h being related to linear polymer dimensions and g to quadratic ones.

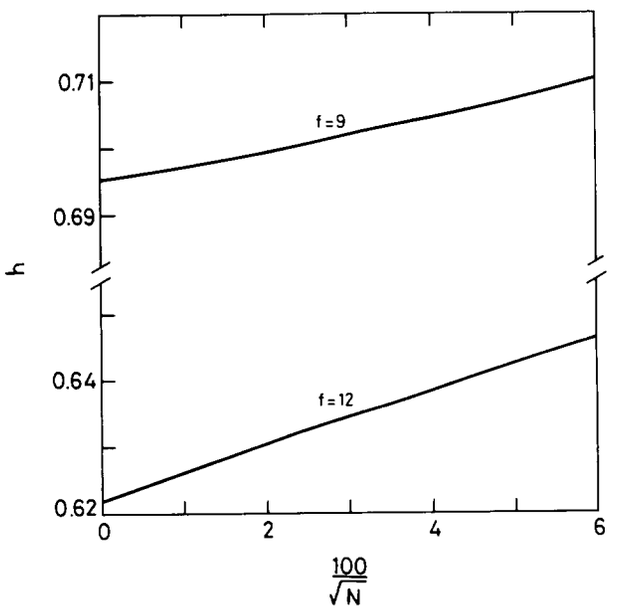

Figure 5 Same as *Figure 4* for the h ratio $h = R_{H,star}/R_{H,lin}$ (see equations (24))

Comparison with experimental data and computer simulations

Experimental results on well characterized monodisperse star polymers in the Θ state with f ranging from 3 to 18, including polystyrene[6], polyisoprene[9] and molten polyethylene[10] stars, suggest that indeed g tends *from above* to an asymptotic value with increasing molecular weight. However, any $N^{-1/2}$ dependence is rather difficult to ascertain due to the relatively small number of data and their scatter. High-molecular-weight values of g are collected in *Table 1*: they are generally indistinguishable from g_∞ for stars having up to about six arms, in agreement with our results in the limit $N \to \infty$, but tend to be larger than g_∞ at larger functionalities ($f = 12$ and 18, possibly $f = 8$ as well). Furthermore, results obtained from different stars with the same f suggest a non-universality of the g ratio, as already pointed out by Douglas *et al.*[15]: in fact, g is larger than g_∞ by about 20% for 12-arm polystyrene[5,6] or 18-arm polybutadiene[11], but it is larger by about 40% for 18-arm polystyrene[5,6], whereas still larger differences are present in the case of 12- or 18-arm polyisoprene[4,9]. However, since the number of bonds per star arm is often not very large (i.e. $N/f < 10^4$, see *Table 1*), experimentally the asymptote may not have been reached yet. This might explain the particularly large g values of molten star polyethylenes[10], which have very small figures of N/f,

Table 1 Values of the g ratio in the Θ state. Theoretical and simulation results are in the limit $N \to \infty$. The N/f range ($\times 10^{-3}$) (N/f = number of repeat units per star arm) is given in parentheses below the corresponding g values; N/f stands for the number of skeletal atoms in experimental samples or the number of lattice points per star arm in Monte Carlo simulations on a lattice (MC)

f	Phantom chain[a]	PS[b]	PIP[c]	PB[d]	PE[e]	MC[f]	MC[g]	MC[h]	Scaling theory[i]
3	0.778	0.63–0.76[6], av. 0.70 (5.9–7.6)	–	–	0.84–0.71[10], av. 0.78 (0.39–0.95)	0.83[19] (≤0.67)	0.79[20] (≤0.90)	–	0.664
4	0.625	0.63[1] (4.3–6.5)	0.65[3] (6.6–29)	–	0.64[10] (1.1)	0.68[19] (≤0.50)	0.68[20] (≤0.90)	0.62[21] (≤0.28)	0.575
5	0.520	–	–	–	–	–	0.55[20] (≤0.90)	0.52[21] (≤0.28)	0.514
6	0.444	0.46[2] (3.6–6.0)	0.46[3] (5–14)	–	–	0.50[19] (≤0.33)	0.48[20] (≤0.90)	0.44[21] (≤0.14)	0.469
8	0.344	–	0.42[4] (13–44) 0.43[9] (32–44)	–	–	0.42[19] (≤0.25)	0.39[20] (≤0.90)	–	0.407
12	0.236	0.28[5,6] (2.7, 8.8)	0.33[4] (19–25) 0.36[9] (19–25)	–	0.29[10] (0.4–1.1)	0.35[19] (≤0.17)	0.28[20] (≤0.90)	–	0.332
18	0.160	0.23[5,6] (9.5)	0.29[9] (12–22)	0.20[11] (3.1–7.8)	0.38[10] (0.09)	–	–	–	0.271

[a] Phantom chain, $g_\infty = (3f-2)/f^2$; see equation (19a)
[b] Atactic polystyrene in cyclohexane at 34.5°C
[c] Polyisoprene in dioxane at 34°C (refs. 3 and 9) or at 33°C (ref. 4)
[d] Polubutadiene in dioxane at 26.5°C
[e] Molten polyethylene at 140°C, partially labelled with deuterium
[f] Simple and face-centred cubic lattice. Θ point criterion: $\langle S^2 \rangle \propto N$. The g values were extrapolated to $N \to \infty$ through $N^{-1} \to 0$, N being 2×10^3 in all cases
[g] Face-centred cubic lattice with g values extrapolated to $N \to \infty$. Θ point criterion: mean-square arm length proportional to N/f
[h] Simple cubic lattice. Extrapolation to $N \to \infty$ through $g = a + b/(N+1)^{1/2} + c/(N+1)$. Θ point criterion: $A_2 = 0$
[i] Scaling theories, using $g \simeq 1.15 f^{-1/2}$, from table III of ref. 13 through fit of experimental data from polyisoprene stars

down to $<10^2$. A further problem arises from possible difficulties with the precise determination of the Θ temperature; in fact, this is depressed in star polymers compared to linear chains, the more so the larger is f and/or the smaller is N/f[24-26].

Up to now, Monte Carlo simulations[19-21] have not provided a clear-cut answer to the problem of whether the limiting g value is actually larger than g_∞. Considering self-avoiding polymers on a lattice with an attractive potential between non-connected segments on adjacent lattice sites, the Θ state can be reproduced by suitably tuning the strength of the potential. It turns out that with increasing molecular weight g decreases to a value *that depends on the criterion chosen to define the* Θ *state*[21]. In fact, if the latter is defined as the state where the mean-square radius of gyration is proportional to the number of bonds, g exceeds g_∞ by a few per cent for any f (up to $\sim 15\%$ for $f=9$, or $\sim 19\%$ for $f=12$[20]), whereas g is equal to g_∞ if the more fundamental criterion of a vanishing second virial coefficient (i.e. $A_2=0$) is adopted (ref. 21, $f\leqslant 6$). Furthermore, in this case an $N^{-1/2}$ dependence is observed, thus basically supporting our theoretical prediction (see equation (17a) and *Figure 1*); furthermore, an additional, weaker dependence from N^{-1} was also detected, yielding a downward curvature qualitatively similar to that found by us (see *Figure 4*). Clearly, it would be of interest to simulate unperturbed stars with a larger functionality adopting the criterion of vanishing A_2 to test whether the same results are still found or if indeed $g>g_\infty$ as the experiments suggest.

Experimental results on the h index are much more scarce. In general, we may say that for 12-arm[5,6] and 18-arm[5] polystyrene h appears to be somewhat larger than h_∞. Like the g ratio, h decreases with increasing molecular weight, but levels off at a value that is definitely larger[6] than h_∞, so that it has been suggested[5] that $h\approx h_\infty^{1/2}$ (we recall that $h<1$ by definition). However, it should be pointed out that R_H attains asymptotic behaviour much more slowly than $\langle S^2\rangle$, the more so the larger is f because of the larger number of short distances across the branch point.

CONCLUDING REMARKS

In this paper we consider the effect of medium-range screened interactions on lightly branched regular stars. These arise from the finite width of the atomic interaction potential: its average value is proportional to the mean-square chain thickness and changes as $\langle r^2\rangle^{-5/2}$, r being the distance between any two atoms, thus yielding a finite chain expansion. The basic result is equation (17a), which shows that the ratio $\langle S^2\rangle/[N\ell^2(3f-2)/f^2]$ changes with molecular weight like $N^{-1/2}$ through the topology-dependent coefficient $\Delta(f)$, and that it tends to an asymptotic limit independent of f for $N\to\infty$; furthermore, this limit is approached from above for $f>4$, since in this case $\Delta(f)$ is negative, unlike for $f<4$. It is remarkable that Monte Carlo simulations on a lattice carried out at a vanishing second virial coefficient do indeed suggest[21] an $N^{-1/2}$ term in the g ratio as the leading correction to g_∞, together with higher-order terms.

According to our results, for a given N the influence of the star topology on α_S^2 is larger the larger is the arm number, hence the shorter is their length, whereas it is negligible in the limit of infinite molecular weight. In this case, the star expansion is affine and equal to that of a linear chain, no dependence on the number of arms being present any more (see equation (16) for $\bar{\alpha}^2$). Conversely, for more heavily branched stars ($f>9$, say) space-filling requirements may become essential in the core region. In particular, we point out that, although three-body interactions involving atoms on one or two arms are basically compensated by two-body attractions at the Θ temperature where the second virial coefficient vanishes, n-body repulsive interactions ($n\geqslant 3$) among atoms on n different arms cannot be compensated in any way. These interactions are particularly effective in increasing the h ratio above h_∞, since, as commented before, h depends rather strongly on short distances, which are most numerous close to the branch point. Therefore, h may reach the asymptotic value h_∞ only for extremely high molecular weight, possibly beyond the accessible range, unlike the g ratio. Scaling approaches describing the star core as a concentrated solution suggest that for large f one should have[13,14] $g\sim f^{-1/2}$ or[20] $g\sim(f-3)^{-1/2}$. Recent Monte Carlo simulations on a lattice[20] indeed suggest a crossover from $g=g_\infty=(3f-2)/f^2$ to $g\sim(f-3)^{-1/2}$ at large f, but in our opinion they are not conclusive in view of the limited ranges both in f and in the arm lengths taken into consideration.

ACKNOWLEDGEMENTS

This work was financially supported by Consiglio Nazionale delle Ricerche (CNR, Italy), Progetto Finalizzato Chimica Fine, and by the Italian Ministry of University and of Scientific and Technological Research (MURST, 40%).

REFERENCES

1 Roovers, J. E. L. and Bywater, S. *Macromolecules* 1972, **5**, 385
2 Roovers, J. E. L. and Bywater, S. *Macromolecules* 1974, **7**, 443
3 Hadjichristidis, N. and Roovers, J. E. L. *J. Polym. Sci., Polym. Phys. Edn.* 1974, **12**, 2521
4 Bauer, B. J., Hadjichristidis, N., Fetters, L. J. and Roovers, J. E. L. *J. Am. Chem. Soc.* 1980, **102**, 2410
5 Roovers, J., Hadjichristidis, N. and Fetters, L. J. *Macromolecules* 1983, **16**, 214
6 Huber, K., Burchard, W. and Fetters, L. J. *Macromolecules* 1984, **17**, 541
7 Huber, K., Burchard, W., Bantle, S. and Fetters, L. J. *Polymer* 1987, **28**, 1990
8 Huber, K., Burchard, W., Bantle, S. and Fetters, L. J. *Polymer* 1987, **28**, 1997
9 Bauer, B. J., Fetters, L. J., Graessley, W. W., Hadjichristidis, N. and Quack, G. F. *Macromolecules* 1989, **22**, 2337
10 Horton, J. C., Squires, G. L., Boothroyd, A. T., Fetters, L. J., Rennie, A. R., Glinka, C. J. and Robinson, R. A. *Macromolecules* 1989, **22**, 681
11 Roovers, J. and Martin, J. E. *J. Polym. Sci. (B) Polym. Phys.* 1989, **27**, 2513
12 Hadjichristidis, N., Guyot, A. and Fetters, L. J. *Macromolecules* 1978, **11**, 668
13 Daoud, M. and Cotton, J. P. *J. Physique* 1982, **43**, 531
14 Birshtein, T. M. and Zhulina, E. B. *Polymer* 1984, **25**, 1453
15 Douglas, J. F., Roovers, J. and Freed, K. F. *Macromolecules* 1990, **23**, 4618
16 Guenza, M., Mormino, M. and Perico, A. *Macromolecules* 1991, **24**, 6168
17 Khokhlov, A. R. *Polymer* 1978, **19**, 1387
18 Khokhlov, A. R. *Polymer* 1981, **22**, 447
19 Mazur, J. and McCrackin, F. *Macromolecules* 1977, **10**, 236
20 Batoulis, J. and Kremer, K. *Europhys. Lett.* 1988, **7**, 683
21 Bruns, W. and Carl, W. *Macromolecules* 1991, **24**, 209
22 Ganazzoli, F., Fontelos, M. A. and Allegra, G. *Polymer* 1991, **32**, 170
23 Allegra, G. and Ganazzoli, F. *Adv. Chem. Phys.* 1989, **75**, 265

24 Ganazzoli, F. and Allegra, G. *Macromolecules* 1990, **23**, 262
25 Allegra, G. and Ganazzoli, F. *Prog. Polym. Sci.* 1991, **16**, 463
26 Cherayil, B. J., Douglas, J. F. and Freed, K. F. *J. Chem. Phys.* 1985, **83**, 5293; 1987, **87**, 3089
27 Allegra, G. and Ganazzoli, F. *Macromolecules* 1991, **24**, 3154
28 Allegra, G. *Macromolecules* 1983, **16**, 555
29 Zimm, B. H. and Kilb, R. W. *J. Polym. Sci.* 1959, **37**, 19
30 Ganazzoli, F., Fontelos, M. A. and Allegra, G. *Polymer* 1992, **33**, 448
31 Allegra, G., Colombo, E. and Ganazzoli, F. *Macromolecules* 1993, **26**, 330
32 Zimm, B. H. and Stockmayer, W. H. *J. Chem. Phys.* 1949, **17**, 1301
33 Stockmayer, W. H. and Fixman, M. *Ann. NY Acad. Sci.* 1953, **11**, 507